

SAPPHIRINE-BEARING SILICA-UNDERSATURATED
GRANULITES FROM FOREFINGER POINT,
ENDERBY LAND, EAST ANTARCTICA:
EVIDENCE FOR A CLOCKWISE *P-T* PATH?

Yoichi MOTOYOSHI¹, Masahiro ISHIKAWA^{2*} and Geoffrey L. FRASER³

¹National Institute of Polar Research, 9-10, Kaga, 1-chome, Itabashi-ku, Tokyo 173

²Institute of Geology and Paleontology, Faculty of Science,
Tohoku University, Sendai 980-77

³Research School of Earth Sciences, Australian National University,
Canberra, ACT 0200, Australia

Abstract: Sapphirine-bearing silica-undersaturated granulites from Forefinger Point in Enderby Land, East Antarctica, preserve a variety of reaction textures suggestive of the prograde segment of the *P-T* evolution followed by nearly isothermal decompression. The granulites are composed of sapphirine, orthopyroxene, cordierite, garnet, spinel, corundum, K-feldspar, biotite and accessory zircon. Petrographical characteristics are i) spinel and corundum occur only as inclusions in sapphirine, ii) relict cordierite and biotite are included in the corundum, and iii) the sapphirine is locally in direct contact with porphyroblastic garnet, and the garnet is occasionally replaced by symplectitic intergrowth of orthopyroxene+sapphirine+cordierite±biotite. Chemographic relations in the FeO-MgO-Al₂O₃-SiO₂ system (FMAS), textural relations and chemical data indicate a clockwise *P-T* trajectory with marked decompression following peak conditions.

1. Introduction

Forefinger Point is situated at the coast of Casey Bay in Enderby Land, East Antarctica (Fig. 1), and is underlain by granulite-facies rocks which are considered to belong to the Rayner Complex (SHERATON *et al.*, 1987). It has been interpreted that a part of the Rayner Complex is a late Proterozoic mobile belt due to reworking of the neighboring Archean Napier Complex (*e.g.* ELLIS, 1983; SHERATON *et al.*, 1980, 1987; HARLEY *et al.*, 1990). In order to characterize the metamorphic evolution of the Rayner Complex, HARLEY *et al.* (1990) investigated the Forefinger Point granulites in detail, and they described a variety of reaction textures mostly involving cordierite as a reaction product in both quartz-bearing and quartz-absent assemblages. On the basis of the reactions, they proposed two-stage decompression, *i.e.* nearly isothermal decompression from 10.5 kbar at above 900°C to 7-8 kbar at 800-850°C, followed by further decompression.

*Present address: Geological Institute, Yokohama National University, Hodogaya-ku, Yokohama 240.

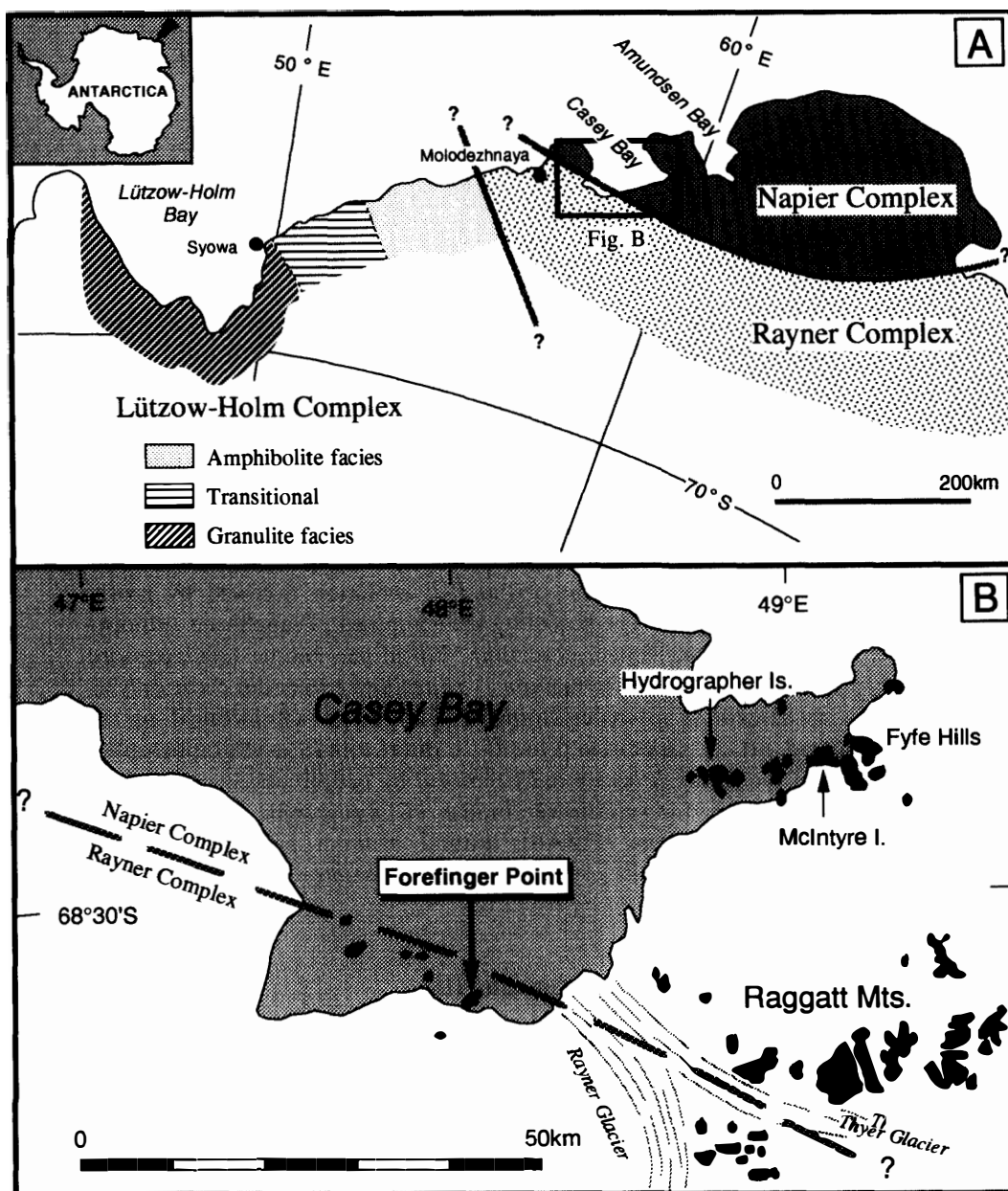


Fig. 1. A: Geological outline in Eastern Queen Maud Land and Western Enderby Land, East Antarctica.
 B: Locality map of Forefinger Point in Casey Bay. The boundary between the Napier and Rayner Complexes is after SHERATON *et al.* (1987).

sion to 4.5 ± 1 kbar at 700–800°C. They considered that the later part of this *P-T* path can be ascribed to overprinting by the late Proterozoic (*c.* 1000 Ma) Rayner metamorphism. With regard to the early decompression, they speculated that it is of Archean age and records thinning of the Napier Complex. In addition to the characteristic reaction textures described by HARLEY *et al.* (1990), MOTOYOSHI *et al.* (1994) newly reported corundum and spinel inclusions as relics in sapphirine in silica-undersaturated rocks. We investigate the petrography of the silica-undersaturated granulites in detail in order to obtain a well-

constrained *P-T* path, with particular emphasis on the possible prograde segment.

2. Petrography and Mineral Chemistry

The silica-undersaturated granulites described in this paper (Sp. 93022211, 93022212, 93022213) occur as blocks in the basement pelitic gneisses, and they contain Spr, Crn, Spl, Opx, Crd, Grt, Bt and Kfs as main constituents. Mineral abbreviations used in this paper are after KRETZ (1983). Because the foliation is almost identical to those of the surrounding gneisses, it is probable that these granulites have undergone deformation and metamorphism simultaneously with the basement gneisses. In view of the unusual mineral assemblages, *i.e.* extremely high Al and Mg bulk compositions, they may be restites formed by partial melting. The characteristic petrographical features of the silica-undersaturated granulites is summarized as follows. Mineral chemistry of the constituent minerals is listed in Table 1. Mineral analysis was performed with an electronprobe microanalyzer JEOL JCXA-733 at the National Institute of Polar Research.

(1) Large Spr crystals, some of them are euhedral, are seen in Kfs as already reported by MOTOYOSHI *et al.* (1994).

(2) Prismatic Spr carries Crn and Spl as inclusions which are never present outside Spr (Figs. 2A and 2B). Spr associated with Crn are peraluminous compositions, more aluminous than $7(\text{Mg, Fe})\text{O} : 9(\text{Al, Fe}^{3+}, \text{Cr})_2\text{O}_3 : 3\text{SiO}_2$ as defined by SCHREYER and ABRAHAM (1975).

(3) Tiny Crd and Bt are recognized as inclusions in Crn (Fig. 2C and 2D).

(4) Pyrope-rich porphyritic Grt ($X_{\text{Mg}} \sim 0.65$) is occasionally associated with prismatic Spr, and no reaction texture is observed between them (Fig. 2B).

(5) Symplectitic intergrowth of Spr+Opx+Crd is locally observed around Grt (Fig. 2E). Grt rim next to the symplectites has lower Mg and higher Mn content relative to the cores (Fig. 3).

(6) Opx in the symplectite contains ~ 8 wt% Al_2O_3 .

(7) Fe^{3+} of Spr and Spl based on stoichiometry is calculated to be low compared to Fe^{2+} .

(8) Abundant Bt is present in the matrix, being associated with Spr (Fig. 2F). The Bt is probably of secondary origin after Opx.

3. Interpretation of the Textures

The earliest stage of the minerals observed in the granulites are tiny euhedral Crd and Bt included in Crn (Figs. 2C and 2D). Crd and Bt also occur in the matrix, for example as members of the symplectites around Grt, but the TiO_2 content of Bt inclusions is much higher (~ 2.7 wt%) than that of Bt in the matrix (Table 1). These Crd and Bt inclusions are interpreted as relics preserved from the previous recrystallization to form Crn at the expense of Bt and Crd. Spr occurs as euhedral crystal in Kfs, implying this phase possibly formed through reactions involving melt. Therefore, two possible reactions are inferred;

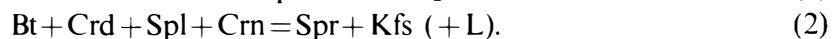


Table 1. Representative mineral analyses.

| | 22211 | | | | | | | 22212 | | | | | | | 22213 | | | | | |
|--------------------------------|--------|--------|--------|--------|--------|--------|-------|--------|--------|--------|-------|--------|--------|--------|--------|--------|--------|-------|--------|--------|
| | Spr(i) | Spr(m) | Crd(i) | Crd(m) | Bt(i) | Bt(m) | Crn | Grt | Spr(i) | Spr(m) | Spl | Opx | Crd | Bt | Grt(c) | Grt(r) | Spr | Opx | Crd | Bt |
| SiO ₂ | 11.81 | 13.63 | 49.69 | 50.02 | 37.05 | 38.24 | 0.00 | 40.21 | 12.15 | 13.73 | 0.04 | 50.11 | 49.77 | 37.27 | 41.02 | 40.03 | 13.27 | 50.24 | 50.29 | 37.59 |
| TiO ₂ | 0.04 | 0.00 | 0.03 | 0.03 | 2.70 | 0.23 | 0.08 | 0.00 | 0.04 | 0.01 | 0.00 | 0.04 | 0.03 | 1.27 | 0.04 | 0.00 | 0.00 | 0.04 | 0.00 | 0.51 |
| Al ₂ O ₃ | 64.45 | 60.56 | 33.42 | 33.73 | 17.59 | 18.61 | 99.21 | 23.53 | 63.91 | 59.89 | 63.96 | 7.58 | 33.77 | 18.83 | 22.91 | 22.21 | 61.77 | 8.21 | 33.73 | 18.62 |
| Cr ₂ O ₃ | 0.01 | 0.00 | 0.01 | 0.00 | 0.01 | 0.00 | 0.00 | 0.00 | 0.00 | 0.00 | 0.00 | 0.00 | 0.03 | 0.02 | 0.00 | 0.00 | 0.06 | 0.07 | 0.00 | 0.03 |
| FeO* | 6.55 | 7.37 | 2.68 | 2.72 | 8.58 | 8.31 | 0.56 | 17.02 | 7.06 | 7.68 | 19.86 | 16.54 | 2.76 | 8.61 | 19.03 | 22.61 | 7.60 | 16.36 | 2.91 | 8.14 |
| MnO | 0.04 | 0.09 | 0.07 | 0.13 | 0.01 | 0.02 | 0.00 | 0.60 | 0.11 | 0.14 | 0.09 | 0.29 | 0.08 | 0.04 | 0.29 | 1.12 | 0.05 | 0.23 | 0.13 | 0.00 |
| MgO | 16.25 | 16.89 | 11.88 | 12.01 | 18.64 | 19.32 | 0.00 | 17.64 | 16.87 | 16.99 | 15.32 | 25.58 | 12.23 | 19.73 | 15.36 | 13.09 | 16.43 | 24.42 | 12.01 | 19.59 |
| CaO | 0.02 | 0.00 | 0.04 | 0.00 | 0.00 | 0.01 | 0.00 | 1.00 | 0.02 | 0.00 | 0.00 | 0.08 | 0.02 | 0.01 | 0.92 | 0.89 | 0.00 | 0.10 | 0.03 | 0.00 |
| Na ₂ O | 0.00 | 0.00 | 0.25 | 0.07 | 0.64 | 0.19 | 0.00 | 0.00 | 0.00 | 0.00 | 0.00 | 0.01 | 0.10 | 0.26 | 0.04 | 0.02 | 0.00 | 0.00 | 0.08 | 0.19 |
| K ₂ O | 0.00 | 0.00 | 0.00 | 0.02 | 8.70 | 9.09 | 0.00 | 0.00 | 0.00 | 0.00 | 0.00 | 0.02 | 0.00 | 8.93 | 0.00 | 0.00 | 0.00 | 0.00 | 0.03 | 9.60 |
| Total | 99.17 | 98.54 | 98.07 | 98.73 | 93.92 | 94.02 | 99.85 | 100.00 | 100.16 | 98.44 | 99.27 | 100.25 | 98.79 | 94.97 | 99.61 | 99.97 | 99.18 | 99.67 | 99.21 | 94.27 |
| O | 20.000 | 20.000 | 18.000 | 18.000 | 22.000 | 22.000 | 3.000 | 12.000 | 20.000 | 20.000 | 4.000 | 6.000 | 18.000 | 22.000 | 12.000 | 12.000 | 20.000 | 6.000 | 18.000 | 22.000 |
| Si | 1.412 | 1.645 | 5.002 | 4.999 | 5.419 | 5.553 | 0.000 | 2.940 | 1.443 | 1.662 | 0.001 | 1.811 | 4.976 | 5.381 | 3.026 | 3.008 | 1.592 | 1.821 | 5.007 | 5.469 |
| Al ^{IV} | 4.588 | 4.355 | 0.998 | 1.001 | 2.581 | 2.447 | - | 0.060 | 4.557 | 4.338 | - | 0.189 | 1.024 | 2.619 | - | - | 4.408 | 0.179 | 0.993 | 2.531 |
| Al ^{VI} | 4.492 | 4.258 | 2.968 | 2.973 | 0.452 | 0.739 | 1.994 | 1.968 | 4.387 | 4.206 | 1.975 | 0.134 | 2.956 | 0.586 | 1.992 | 1.968 | 4.326 | 0.172 | 2.966 | 0.663 |
| Ti | 0.004 | 0.000 | 0.002 | 0.002 | 0.297 | 0.025 | 0.001 | 0.000 | 0.004 | 0.001 | 0.000 | 0.001 | 0.002 | 0.138 | 0.002 | 0.000 | 0.000 | 0.001 | 0.000 | 0.056 |
| Cr | 0.001 | 0.000 | 0.001 | 0.000 | 0.001 | 0.000 | 0.000 | 0.000 | 0.000 | 0.000 | 0.000 | 0.000 | 0.002 | 0.002 | 0.000 | 0.000 | 0.006 | 0.002 | 0.000 | 0.003 |
| Fe ³⁺ | 0.095 | 0.098 | - | - | 0.157 | 0.151 | 0.007 | - | 0.171 | 0.131 | 0.024 | 0.080 | - | 0.156 | 0.014 | 0.040 | 0.076 | 0.003 | - | 0.149 |
| Fe ²⁺ | 0.559 | 0.646 | 0.226 | 0.227 | 0.893 | 0.858 | - | 1.041 | 0.531 | 0.647 | 0.411 | 0.420 | 0.231 | 0.884 | 1.160 | 1.380 | 0.686 | 0.493 | 0.242 | 0.842 |
| Mn | 0.004 | 0.004 | 0.006 | 0.011 | 0.001 | 0.002 | 0.000 | 0.037 | 0.011 | 0.014 | 0.002 | 0.009 | 0.007 | 0.005 | 0.018 | 0.071 | 0.005 | 0.007 | 0.011 | 0.000 |
| Mg | 2.896 | 3.038 | 1.782 | 1.789 | 4.063 | 4.181 | 0.000 | 1.923 | 2.986 | 3.066 | 0.598 | 1.378 | 1.822 | 4.246 | 1.689 | 1.466 | 2.939 | 1.319 | 1.782 | 4.247 |
| Ca | 0.003 | 0.000 | 0.004 | 0.000 | 0.000 | 0.002 | 0.000 | 0.078 | 0.003 | 0.000 | 0.000 | 0.003 | 0.002 | 0.002 | 0.073 | 0.072 | 0.000 | 0.004 | 0.003 | 0.000 |
| Na | 0.000 | 0.000 | 0.049 | 0.014 | 0.182 | 0.054 | 0.000 | 0.000 | 0.000 | 0.000 | 0.000 | 0.001 | 0.019 | 0.073 | 0.006 | 0.003 | 0.000 | 0.000 | 0.015 | 0.054 |
| K | 0.000 | 0.000 | 0.000 | 0.003 | 1.623 | 1.684 | 0.000 | 0.000 | 0.000 | 0.000 | 0.000 | 0.001 | 0.000 | 1.645 | 0.000 | 0.000 | 0.000 | 0.000 | 0.004 | 1.782 |
| \bar{X}_{Mg} | 0.838 | 0.825 | 0.887 | 0.887 | 0.820 | 0.830 | - | 0.649 | 0.849 | 0.826 | 0.593 | 0.766 | 0.887 | 0.828 | 0.593 | 0.515 | 0.811 | 0.728 | 0.880 | 0.835 |

i - as inclusion; m - in the matrix; c - core; r - rim.

Fe³⁺ is calculated based on stoichiometry.

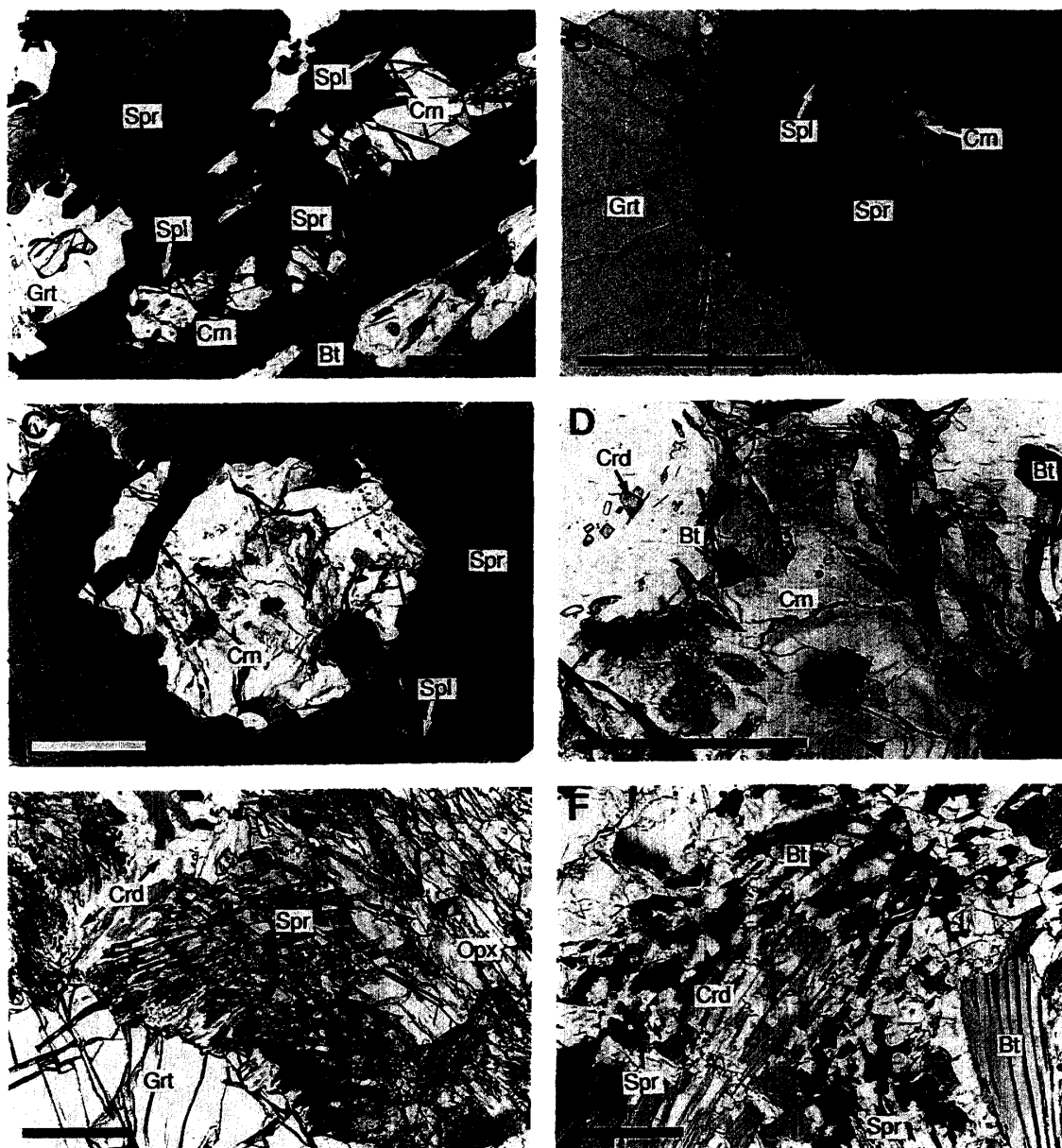


Fig. 2. Photomicrographs of silica-undersaturated granulites from Forefinger Point. Scale bars are all 1 mm.

- A. Crn + Spl inclusions in Spr. Crn and Spl are never present outside Spr (Sp. 93022213).
- B. Direct contact of Grt and Spr. Spr carries Crn and Spl as inclusions. Grt is free from inclusions (Sp. 93022212).
- C. Crn in Spr also carries inclusions in it (Sp. 93022211).
- D. Tiny Crd and Bt as inclusions in Crn (Sp. 93022211).
- E. Symplectitic intergrowth of Spr + Opx + Crd + Bt around Grt (Sp. 93022213).
- F. Spr + Crd + Bt assemblage in the matrix (Sp. 93022211).

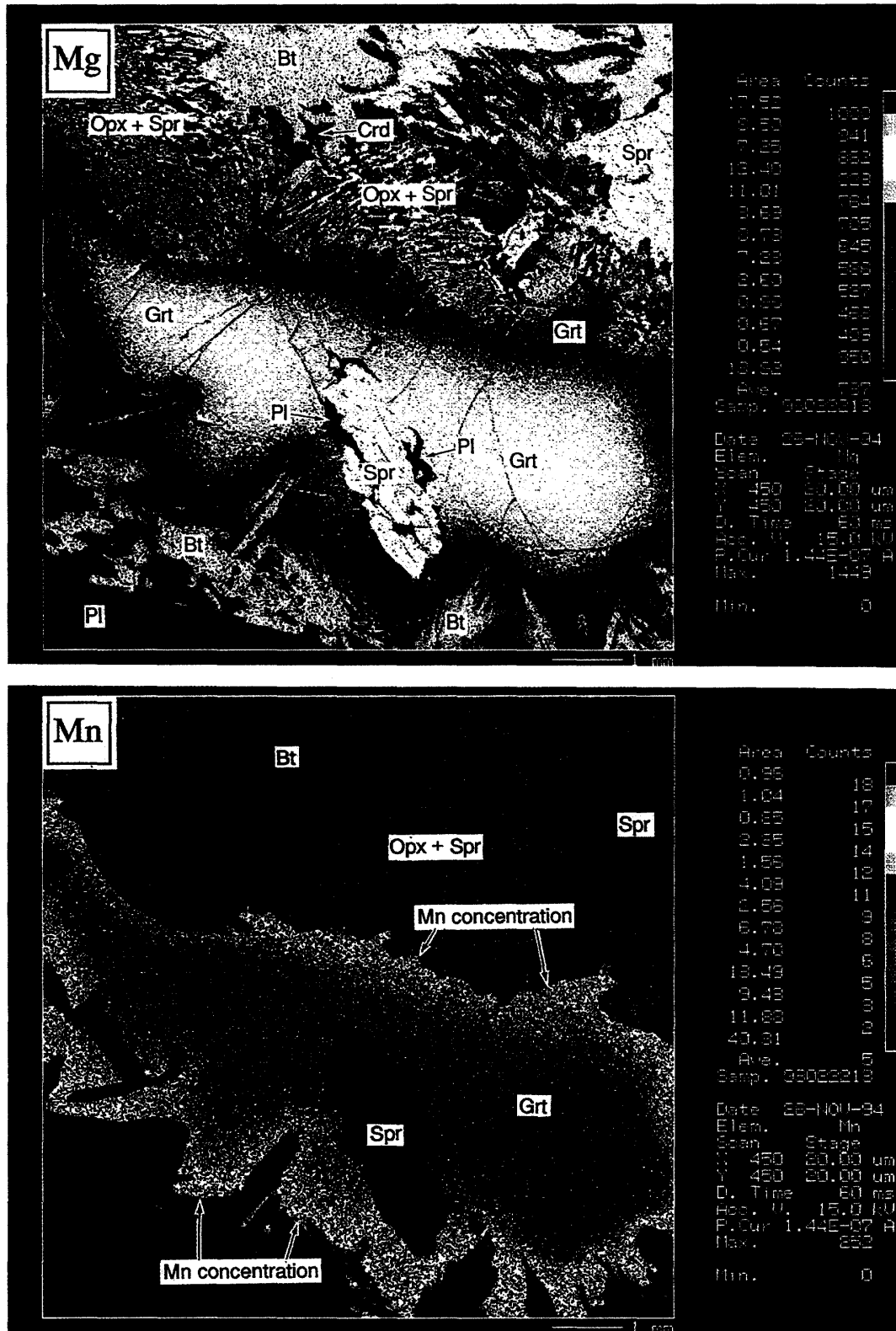


Fig. 3. WDS-compositional mapping for Mg (top) and Mn (bottom) concentration in Grt and the associated phases. Note marked Mg-depletion and Mn-concentration along the Grt rim.

Alternatively, in case Spr has formed independently, the following reaction is inferred;



which is divariant in FMAS and has a negative slope with Spr on high-temperature side on a P - T space (HENSEN, 1987).

As is mentioned already, Spr and Grt show mutual contact to each other, and there is no distinctive reaction texture, suggesting that they are in stable coexistence (Fig. 2B). On the P - T grid, the stability field of Grt+Spr occupies a higher P - T domain relative to reaction (3), thus the prograde P - T path involves increasing pressure with increasing temperature.

The maximum P - T conditions are represented by Opx+Sil-bearing assemblages observed in nearby pelitic granulites (HARLEY *et al.*, 1990; MOTOYOSHI *et al.*, 1994). It is not possible to specify the P - T conditions for that assemblage, but 10 ± 1.5 kbar at around 900°C have been proposed based on the petrogenetic grid. It is worth noting that no Spr+Qtz relics have been reported from the Forefinger Point granulites. As is well known, Spr+Qtz is a diagnostic mineral assemblage in the high-grade zone of the neighboring Napier Complex, and its absence at Forefinger Point suggests that the maximum T conditions of the Forefinger Point granulites must have been lower than those of the highest-grade granulites of the Napier Complex (*e.g.* HARLEY and HENSEN, 1990).

The decompressional stage is demonstrated by formation of symplectitic intergrowth of Opx+Spr+Crd at the expense of Grt as in Sp. 93022213 (Fig. 2E and Fig. 3), and this

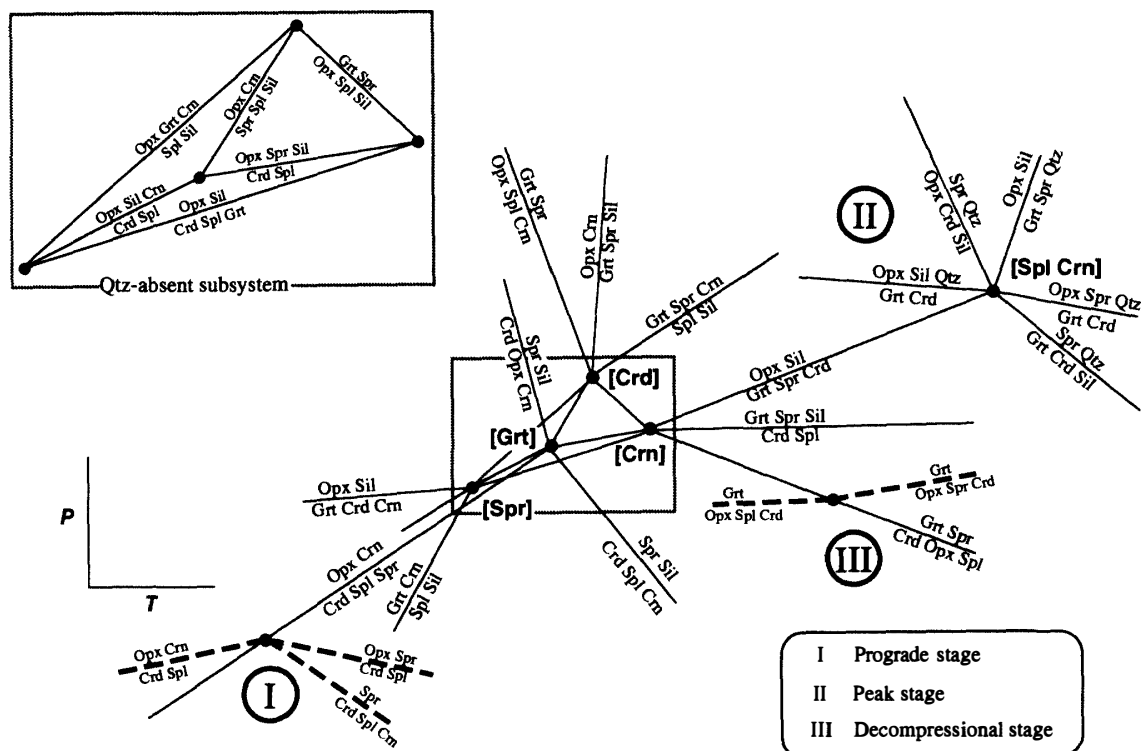
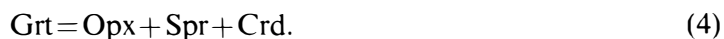


Fig. 4. Proposed P - T path for the silica-undersaturated granulites from Forefinger Point. The FMAS grid is after HENSEN (1987). The heavy dashed lines are divariant reactions, and the rest are univariant boundaries. See text for further explanation.

texture reflects the decompressional reaction;



This reaction is well-documented by WDS-compositional mapping for Mg- and Mn-concentration in Grt and the neighboring phases (Fig. 3). Marked Mg-depletion and Mn-enrichment is observed along the Grt rim due to formation of the symplectites. This clearly indicates that the symplectites have formed at the expense of pyrope component of Grt. It is worth noting that no distinctive chemical gradient is observed between Spr inclusion and the surrounding Grt, suggesting that there were at least two stages of the Spr-forming reactions.

These lines of evidence are indicative of a prograde sequence of recrystallization, *i.e.* increasing temperature with increasing pressure to reach the maximum *P-T* conditions at above 900°C at 10 ± 1.5 kbar, followed by decompressional Grt-consuming reactions to form the Opx + Spr + Crd symplectite. In view of the high Al₂O₃ content of Opx in the symplectite, the reaction (4) has taken place under relatively high-temperature conditions, implying near-isothermal decompression. Combining the present data with the well-documented decompressional *P-T* path by HARLEY *et al.* (1990) and MOTOYOSHI *et al.* (1994) for the Forefinger Point granulites, we propose a clockwise *P-T* evolution as presented in Fig. 4.

4. Implication for the Metamorphic Evolution of the Rayner Complex

On the basis of mineral textures in the granulites, the *P-T* trajectory followed by rocks of Forefinger Point is presented in Fig. 4. This *P-T* trajectory has a clockwise sense, which is seen in a number of orogenic belts in East Antarctica. Well-constrained *P-T* paths have been reported from several localities in the Rayner Complex and the Lützow-Holm Complex, most of them being characterized by relatively isothermal decompressional trajectories (HARLEY and HENSEN, 1990, and references therein; HARLEY and FITZSIMONS, 1991; THOST *et al.*, 1991; KAWASAKI *et al.*, 1993). HARLEY *et al.* (1990) pointed out that the very high *P-T* conditions recorded in the Forefinger Point granulites are unusual in the context of granulites in this part of East Antarctica, except for the Napier Complex. Their basic idea is that the high *P-T* rocks and decompressional *P-T* path are related to the *P-T* evolution of the Napier Complex, and the initial decompression occurred in Archean, followed by the second decompression which was related to the Rayner metamorphism. However, recent SHRIMP dating on zircons in a Grt- and Sil-bearing metapelite from Forefinger Point yielded dominantly Paleozoic ages (~500 Ma), rather than Archean (SHIRAIISHI, unpublished data). These results imply that the Forefinger Point granulites have undergone much younger events than previously suspected, and may constitute a part of the so-called "500 Ma" zone in this part of East Antarctica.

Acknowledgments

We express our sincere thanks to H. KOJIMA for his assistance in microprobe analyses using JEOL JXA-733 at the National Institute of Polar Research, and to H. ISHIKAWA and S. SUZUKI for performing WDS-compositional mapping using JEOL JXA-8600 at Kochi

University. K. SHIRAIISHI is acknowledged for his fruitful discussion and providing us unpublished data on SHRIMP dating. Thanks are extended to Y. HIROI, M. ARIMA and E.S. GREW for their careful and constructive reviews.

References

- ELLIS, D.J. (1983): The Napier and Rayner complexes of Enderby Land, Antarctica : Contrasting styles of metamorphism and tectonism. *Antarctic Earth Science*, ed. by R.L. OLIVER *et al.* Canberra, Aust. Acad. Sci., 20-24.
- HARLEY, S.L. and FITZSIMONS, I.C.W. (1991): Pressure-temperature evolution of metapelitic granulites in a polymetamorphic terrane: The Rauer Group, East Antarctica. *J. Metamorph. Geol.*, **9**, 231-243.
- HARLEY, S.L. and HENSEN, B.J. (1990): Archaean and Proterozoic high-grade terranes of East Antarctica (40-80°E): A case study of diversity in granulite facies metamorphism. *High-temperature Metamorphism and Crustal Anatexis*, ed. by J.R. ASHWORTH and M. BROWN. London, Unwin Hyman, 320-370.
- HARLEY, S.L., HENSEN, B.J. and SHERATON, J.W. (1990): Two-stage decompression in orthopyroxene-sillimanite granulites from Forefinger Point, Enderby Land, Antarctica: implications for the evolution of the Archaean Napier Complex. *J. Metamorph. Geol.*, **8**, 591-613.
- HENSEN, B.J. (1987): *P-T* grids for silica-undersaturated granulites in the systems MAS ($n+4$) and FMAS ($n+3$): Tools for the derivation of *P-T* paths of metamorphism. *J. Metamorph. Geol.*, **5**, 255-271.
- KAWASAKI, T., ISHIKAWA, M. and MOTOYOSHI, Y. (1993): A preliminary report on cordierite-bearing assemblages from Rundvågshetta, Lützow-Holm Bay, East Antarctica: Evidence for a decompressional *P-T* path? *Proc. NIPR Symp. Antarct. Geosci.*, **6**, 47-56.
- KRETZ, R. (1983): Symbols for rock-forming minerals. *Am. Mineral.*, **68**, 277-279.
- MOTOYOSHI, Y., ISHIKAWA, M. and FRASER, G.L. (1994): Reaction textures in granulites from Forefinger Point, Enderby Land, East Antarctica: An alternative interpretation on the metamorphic evolution of the Rayner Complex. *Proc. NIPR Symp. Antarct. Geosci.*, **7**, 101-114.
- SCHREYER, W. and ABRAHAM, K. (1975): Peraluminous sapphirine as a metastable reaction product in kyanite-gedrite-talc schist from Sar e Sang, Afganistan. *Mineral. Mag.*, **40**, 171-180.
- SHERATON, J.W., OFFE, L.A., TINGEY, R.J. and ELLIS, D.J. (1980): Enderby Land, Antarctica : An unusual Precambrian high grade metamorphic terrain. *J. Geol. Soc. Aust.*, **27**, 1-18.
- SHERATON, J.W., TINGEY, R.J., BLACK, L.P., OFFE, L.A. and ELLIS, D.J. (1987): Geology of Enderby Land and western Kemp Land, Antarctica. *BMR Bull.*, 223, 51 p.
- THOST, D.E., HENSEN, B.J. and MOTOYOSHI, Y. (1991): Two-stage decompression in garnet-bearing mafic granulites from Sjøstrene Island, Prydz Bay, East Antarctica. *J. Metamorph. Geol.*, **9**, 245-256.

(Received April 14, 1995; Revised manuscript received June 30, 1995)